

Original Article | ISSN (0): 2582-631X

DOI: 10.47857/irjms.2025.v06i04.06096

# Real-Time Sensor-Less Vector Control of Induction Motor Drive Using Model Reference Adaptive System

Vivek Pahwa\*

Department of Electrical and Electronics Engineering, University Institute of Engineering and Technology, Panjab University, Chandigarh, Chandigarh, India-160014. \*Corresponding Author's Email: v1974pahwa@gmail.com

#### Abstract

In today's competitive and advanced motion control industries, any designed controller is expected to provide precise speed control and reduced time-to-market for its practical deployment. In the current study, a Model Reference Adaptive System based sensor-less vector controlled induction motor drive system is meticulously designed and simulated in time-domain using an offline environment namely MATLAB/SIMULINK software utilizing a rotor reference frame. The suggested controller's ability to precisely follow the reference speed even at 33% of its rated speed demonstrates its superiority. The efficacy of the proposed strategy is further substantiated through an examination in the s-domain. However, the signals generated by this controller are not real-time clock synchronized due to a large computation burden of up to 20 times, even when utilizing the latest configured PC with *i7* processor. Thus, the model is transformed from offline to online model with a field programmable gate array based OPAL-RT real-time-simulator using Rapid-Control-Prototyping strategy. Due to parallel processing of the simulator, the proposed set-up produces real-time clock synchronized signals by reducing the computation load to the required value of one. The similarity of offline and online results not only validates the proposed model, but the development process can help researchers to analyze potential design flaws early, reducing both costs and time-to-market, boosting practical implementation of the proposed controller in reduced time.

**Keywords:** Induction Machine, Model-Reference-Adaptive-System, Rapid-Control-Prototyping, Real-Time-Simulator.

#### Introduction

Induction motors are extensively employed in industrial applications owing to their durability, cost-effectiveness, and exceptional efficiency (1, 2). Nevertheless, the control of these machines poses significant challenges due to their inherently non-linear and interdependent characteristics. Vector control technique has emerged as an effective solution for precise speed control of induction motor. This control method often relies on speed sensors, which can increase costs, reduce reliability, and limit the application of the drive system in certain environments (3). To address issues. various sensor-less techniques based on back-emf estimation, high frequency injection, model estimation, specialized schemes and Model Reference Adaptive System (MRAS) have gained popularity during the last two decades (4-9). Among these, MRAS has shown potential due to its adaptive nature and fast dynamic response. The MRAS-based speed

estimation compares the outputs of a reference model with an adaptive model, adjusting until the error between them converges to zero (9).

Furthermore, MRAS observers estimate rotor speed and position using machine currents, allowing for effective vector control in both gridconnected and stand-alone operations (10, 11). MRAS-based sensor-less control can be combined with other techniques to enhance performance. For instance, integrating sliding mode observers improve robustness against uncertainties and parameter variations (12). Additionally, the use of adaptive-gain super twisting sliding mode speed controllers can provide better speed tracking under load torque variations (13). Some studies have also explored the combination of MRAS with Adaptive Neuro-Fuzzy Inference Systems (ANFIS) to further improve dynamic performance and reduce sensitivity to parameter variations (14).

This is an Open Access article distributed under the terms of the Creative Commons Attribution CC BY license (http://creativecommons.org/licenses/by/4.0/), which permits unrestricted reuse, distribution, and reproduction in any medium, provided the original work is properly cited.

(Received 05th June 2025; Accepted 23rd September 2025; Published 30th October 2025)

The method's adaptability to parameter variations and its ability to be combined with other control techn iques make it a versatile solution for industrial applications requiring precise speed control without mechanical sensors. However, these complex combinations results in increased computational burden, which deters its usefulness in real-time environment. Out of three reference frames i.e. stator reference frame, rotor reference frame and synchronously rotating reference frame, selection of an appropriate reference frame for the implementation of intricate schemes such as MRAS based sensor-less vector control of induction machines is of paramount importance (1, 15,16). The rotor reference frame (RRF) has been identified as suitable for fast and accurate dynamic response of the field-oriented control of rotor-tied Doubly Fed Induction Generator for wind energy conversion scheme. The rotor phase 'a' current of DFIG is superimposed on rotor q-axis current, which allows the decoupling of flux and torque components, enabling independent control of these parameters (16). Recently, a Minimum-Order Sensor-less Induction Motor Control Method has been devised for the regulation of induction machines. The outcomes from both slow and rapid reversal experiments indicate that the design is  $proficient \, in \, achieving \, dynamic \, performance \, while \,$ ensuring stable operation in proximity to zero frequency. Although the results are promising, the implementation poses challenges due to the necessity for a specialized experimental setup, which escalates both cost and complexity (17).

Therefore, the integration of MRAS-based sensorless vector control represents a promising direction for improving the performance and practical deployment of induction motor drives in modern industrial applications. This approach offers speed precise control, reduced implementation time, and enhanced adaptability to meet the competitive market demands. Moreover, most of the control algorithms developed and simulated in offline environments using software package like MATLAB/Simulink, their practical implementation challenging. This is because the control signals generated in offline simulations are not synchronized with real-time clocks (18).

To bridge this gap, researchers have explored the use of digital real-time simulation (DRTS) platforms. These platforms enable the generation of control signals synchronized with real-time clocks. Rapid Control Prototyping (RCP), a specific implementation of Hardware-in-the-Loop (HIL) simulation, has emerged as a promising approach for validating control algorithms and reducing development time and costs (18-24). This process allows the practical implementation of complex control algorithms by reducing the computational burden while minimizing plant stoppage time and enhancing deployment in competitive industrial environments.

In light of the aforementioned considerations, a Model Reference Adaptive System-based sensorless vector-controlled induction motor drive system has been meticulously designed and simulated within the time domain utilizing the MATLAB/SIMULINK environment. The proposed controller adeptly tracks the reference speed even at one-third of its rated velocity. Consequently, the model has transitioned from an offline framework to an online paradigm, employing a fieldprogrammable gate array-based OPAL-RT-4510 real-time simulator through a Rapid-Control-Prototyping strategy. Thanks to the parallel processing capabilities of the simulator, the proposed setup generates real-time clocksynchronized signals while significantly reducing the computational load to the essential value of one.

# Methodology

The system considered for this work shown in Figure 1 has a power and a control circuit. In the power circuit, a grid-simulator feeds the desired variable supply to the induction motor for precise speed control. Whereas, the control circuit generates the pulses to the grid-simulator, after comparing the motor and reference signals. The control is based on sensor-less vector control theory. In this section, the dynamic modelling of the induction machine, its feed forward vector control along with the description of the model reference adaptive system (MRAS), determination of induction machine parameters, and its control and transformation from offline to online environment are discussed.

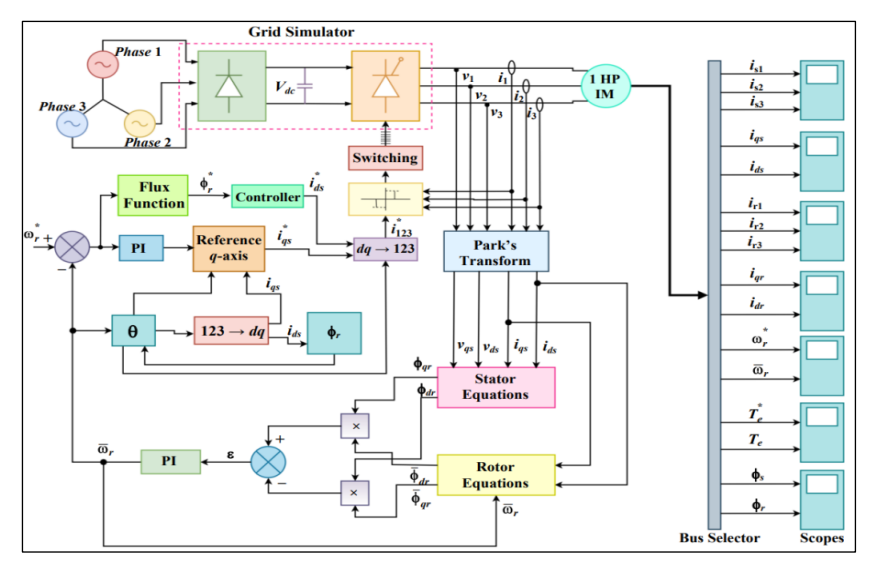


Figure 1: Block Diagram for Sensor-Less Vector Control of Induction Motor Drive

# **Dynamic Modelling of Induction Machine**

Considering the d-q model (1) of the induction machine in the reference frame rotating at a synchronous speed  $\omega_e$ ,

$$v_{qs} = R_s i_{qs} + \frac{d\phi_{qs}}{dt} + \omega_e \phi_{ds}$$
 [1]

$$v_{ds} = R_s i_{ds} + \frac{d\phi_{ds}}{dt} - \omega_e \phi_{qs}$$
 [2]

For a squirrel cage induction machine  $v_{ds} = v_{qs} = 0$ , thus

$$v_{qr} = 0 = R_r i_{qr} + \frac{d\phi_{qr}}{dt} + (\omega_e - \omega_r)\phi_{dr}$$
 [3]

$$v_{dr} = 0 = R_r i_{dr} + \frac{d\phi_{dr}}{dt} - (\omega_e - \omega_r)\phi_{qr}$$
[4]

The electromagnetic torque  ${}'T_e{}'$  produced in the induction machine is given as

$$T_{e} = 1.5 p \frac{L_{m}}{L_{r}} (\phi_{dr} i_{qs} - \phi_{qr} i_{ds})$$
 [5]

Where

$$\phi_{qs} = L_{s}i_{qs} + L_{m}i_{qr} 
\phi_{ds} = L_{s}i_{ds} + L_{m}i_{dr} 
\phi_{qr} = L_{r}i_{qr} + L_{m}i_{qs} 
\phi_{dr} = L_{r}i_{dr} + L_{m}i_{ds}$$
[6]

The nomenclature of the symbols used is given as:  $v_{qs}$  = quadrature axis stator voltage,  $v_{ds}$  = direct axis stator voltage,  $v_{dr}$  = quadrature axis rotor voltage,  $v_{dr}$  = direct axis rotor voltage,  $R_s$  = stator winding resistance,  $L_s$  = stator winding leakage inductance,  $L_m$  = magnetizing inductance,  $R_r$  = rotor winding resistance referred to the stator,  $L_r$  = rotor winding leakage inductance referred to the stator,  $\omega_s$  =

synchronous speed for ds-qs axes,  $\omega_r$  = rotor speed, p = number of pole pairs,  $\phi_{qs}$  = quadrature axis stator flux,  $\phi_{ds}$  = direct axis stator flux,  $\phi_{qr}$  = quadrature axis rotor flux, and  $\phi_{dr}$  = direct axis rotor flux.

The speed  $\omega_r$  in equations [3] and [4] cannot typically be assumed constant, it relates to the torque as

$$T_e - T_L = J \frac{d\omega_r}{dt}$$
 [7]

where  $T_L$  = load torque, and J = moment of inertia of the machine.

#### **Feed forward Vector Control**

Rearranging the terms in [6], the following expressions can be obtained

$$i_{qr} = \frac{1}{L_r} \phi_{qr} - \frac{L_m}{L_r} i_{qs}$$
 [8]

$$i_{dr} = \frac{1}{L_{r}} \phi_{dr} - \frac{L_{m}}{L_{r}} i_{ds}$$
 [9]

Substituting the equations [8] and [9] in [3] and [4] respectively, yields

$$\frac{d\phi_{qr}}{dt} + \frac{R_r}{L_u}\phi_{qr} - \frac{R_rL_m}{L_u}i_{qs} + (\omega_e - \omega_r)\phi_{dr} = 0$$
[10]

$$\frac{d\phi_{dr}}{dt} + \frac{R_r}{L_u}\phi_{dr} - \frac{R_rL_m}{L_u}i_{ds} - (\omega_e - \omega_r)\phi_{qr} = 0$$
[11]

For decoupled control,  $\phi_{qr}$  is set to zero to simplify the control strategy and ensure independent regulation of torque and flux. Since  $\phi_{qr} = 0$ , which implies that  $d\phi_{qr}/dt = 0$ . As a result, the total rotor flux reduces to  $\phi_r = \phi_{qr}$ , ensuring that only the direct-axis component contributes to the rotor flux. With this simplification, the following expressions can be easily obtained.

$$\omega_e - \omega_r = \frac{R_r L_m}{\phi_L L_n} i_{qs}$$
 [12]

$$\frac{d\phi_r}{dt} = -\frac{R_r}{L_n}\phi_r + \frac{R_r L_m}{L_n}i_{ds}$$
 [13]

$$T_e = 1.5 p \frac{L_m}{L} (\phi_r i_{qs})$$
 [14]

# Speed Estimation Using Model Referencing Adaptive System (MRAS)

The Model Reference Adaptive System (MRAS) is a used for estimating the speed of an induction motor. It operates by comparing the outputs of a reference model with those of an adaptive model until the error between them converges to zero (9). The block diagram illustrating the MRAS-based speed estimation of an induction motor is shown in

Figure 2. With the speed signal  $\omega_r$  available, the model calculates the flux components from the stator current inputs. When the correct speed is determined, the fluxes estimated by the reference model align with those from the adaptive model, i.e.,  $\varphi_{qr} = \underline{\varphi_{qr}}$  and  $\underline{\varphi_{dr}} = \underline{\varphi_{dr}}$ , where  $\underline{\varphi_{qr}}$  and  $\underline{\varphi_{dr}}$  are the outputs of the adaptive model. The following expression for speed estimation is derived using Popov's criterion for hyper-stability:

$$\overline{\omega_r} = \varepsilon \left( K_p + \frac{K_i}{s} \right)$$
 [15]

Where

$$\varepsilon = \phi_{ar} \overline{\phi_{dr}} - \phi_{dr} \overline{\phi_{ar}}$$
 [16]

It is evident from the above equation that if  $\varphi_{qr}=\ \underline{\varphi_{qr}}$  and  $\varphi_{dr}=\ \underline{\varphi_{dr}}$  , then  $\epsilon$  = 0.

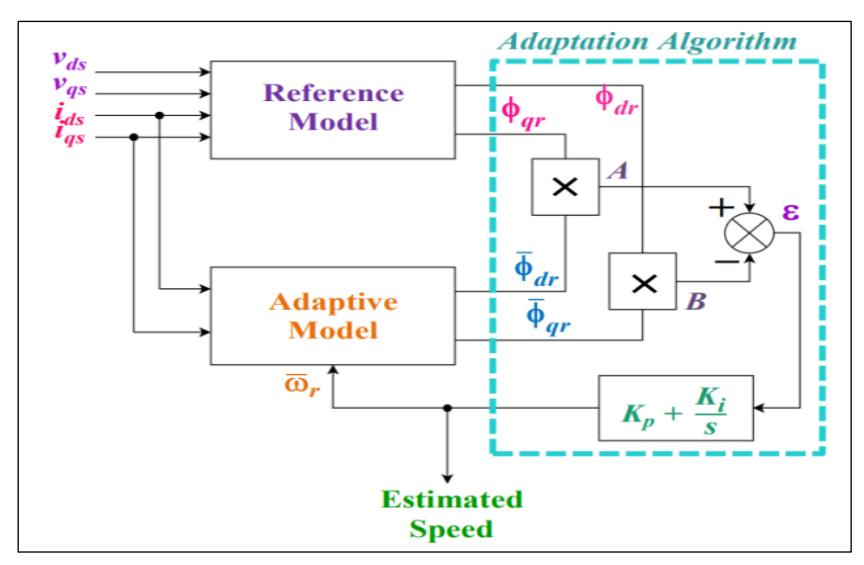


**Figure 2:** Speed Estimation Using MRAS

# Parameters of Induction Machine and its Control

This subsection deals with the parameter determination of induction machine and its control scheme. The parameters of induction machine have been determined using the blocked rotor test,

the stator resistance test and the no-load test (1). However, the moment of inertia which is a critical component for machine dynamics has been determined using acceleration test (25). The induction machine used is three-phase 440 V, 50 Hz, 4 poles, 1-hp motor with its calculated parameters are given below:

Per phase stator resistance  $R_s = 10.75 \Omega$ , Per phase rotor resistance  $R_r = 11.06 \Omega$ , Per phase stator inductance  $L_s = 0.048 H$ , Per phase rotor inductance  $L_r = 0.048 H$ , Per phase mutual inductance  $L_m = 0.904 H$ , and Moment of inertia of the rotor  $J = 0.0124 \ kg$ - $m^2$ 

The values of the capacitance, resistance, activation voltage, and shutdown voltage of the d.c. bus are  $200~\mu F$ ,  $542~\Omega$ , 636~V, and 596~V respectively. Further, the values of the proportional and integral constant used in the speed regulator are 5 and 10 respectively, and those for the flux controller are 100 and 30. These parameters have been calculated using the Zeigler-Nicholas method (26).

# **Transformation from Offline to Online Environment Using RCP**

The model as illustrated in Figure 1 has been developed in an offline environment using MATLAB/Simulink software and generates the unsynchronized control signals. Therefore, the conversion of this model to an online environment

is essential. A flowchart depicting the conversion process is shown in Figure 3 where the host PC contains the command authorities of the real-time simulation, and the model for the desired controlled system is designed in the MATLAB/Simulink environment. The designed model is then converted into subsystems, i.e., Master subsystem (SM) and Console subsystem (SC).

The SC contains the monitoring components which are required during the simulation and the rest of the model resides in the SM. This converted model is then burnt into the real-time simulator OPAL-RT (OP4510) via its interfacing software RT Labs. The OPAL-RT outputs are connected to the grid simulator external control via a DB-37 connector.

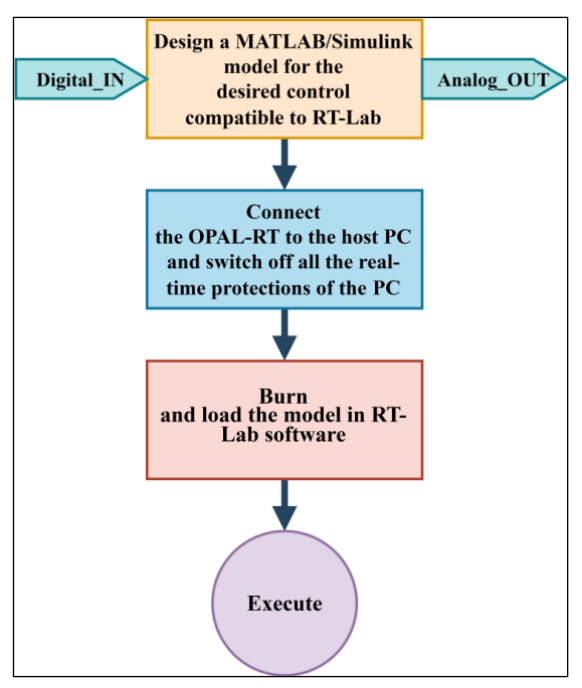


Figure 3: Flowchart Showing the Transformation from Offline to Online Environment

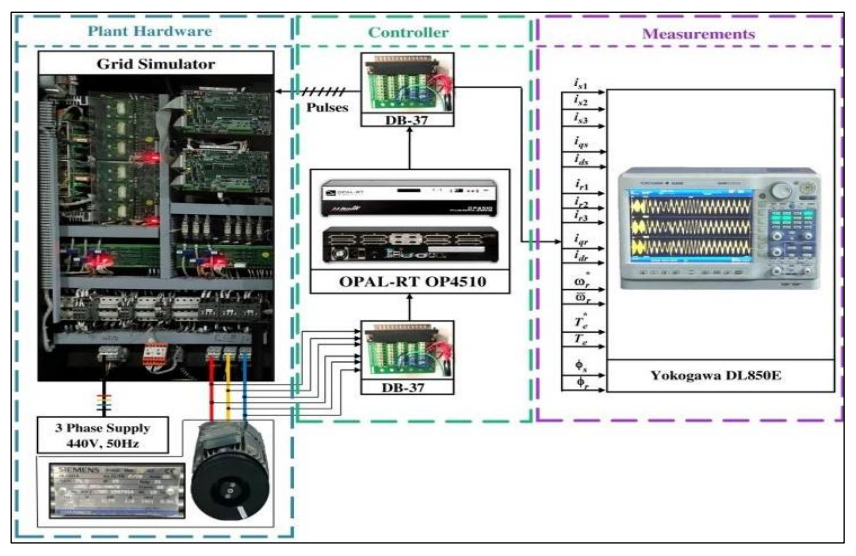


Figure 4: Experimental Set-Up in Online Environment Using the RCP Technique

After burning the model in RT Lab software, a connection between the host PC and the real-time simulator is established via Ethernet. The model is then interfaced with the hardware setup of the grid simulator and the results are observed with the digital storage oscilloscope as shown in Figure 3 and Figure 4.

#### **Results and Discussion**

The model of the system given in Figure 1 is developed in MATLAB/Simulink environment using equations [1] to [16]. The calculated parameters of the 1-hp motor and drive system are given in the previous section. The simulation was

run for 8.2 seconds. At 1 second, the machine is started with a ramp of 500 rpm/s with an applied load torque of 2.5 Nm. The speed set point is 500 rpm and remains constant for the next 2 seconds. After 2 seconds, the machine is decelerated with the same ramp. For the remaining period, the machine runs at zero speed. The simulated results of various important variables are given from Figure 5 to Figure 11.

It can be observed from the Figure 5(A) and Figure 5(B) that the actual rotor speed follows the reference speed accurately, without any oscillations and, moreover, the steady-state error between reference and actual speed is zero,

showing the superiority of the MRAS controller. Thus, there is no need for any sensor. Another noticeable point is that the speed remains constant even at 500 rpm, which is the unstable region of the induction machine showing the superiority of vector control. The dynamic variation of electromagnetic torque with reference load torque is illustrated in Figure 6(B) and 6(A) respectively. It is to noted here that the time span chosen here is 2.2 sec for clarity. Further, it can be seen from these figures that electromagnetic torque follows the load torque adequately. The settling time for torque is 0.01 seconds at starting, and it remains below 0.01 seconds during subsequent alterations. Similarly, the peak-to-peak variation is 10 Nm at starting, diminishing to 6 Nm or less during all other adjustments.

The stator currents of phases 'a, b and c' have been shown in Figures 7(A), 7(B) and and 7(c) respectively and are 120 degrees displaced from each other. It is evident from the Figures 7(A) that the initial current of phase 'a' is constrained to 5 A (peak-to-peak) due to the implemented speed ramp; consequently, both the size and cost of the inverter will be reduced significantly. In contrast, in the absence of this ramp, the typical starting current of an induction machine could escalate to 5 to 6 times its rated current, increasing the size and cost of the inverter (1).

The three-phase currents illustrated in Figure 7 have been transmuted into the qd-axis representation, as demonstrated in Figures 8(A) and 8(B), employing Park's transformation. These qd-axes are oriented 90 degrees apart from one another, exemplifying the vector-controlled operation of the induction machine drive system. Similarly, the three-phase rotor currents, displaced by 120 degrees, are depicted in Figures 9(A), 9(B), and 9(C). The transformed qd-axes for the rotor phases are presented in Figures 10(A) and 10(B).

Observation of waveforms in Figure 7(A) and Figure 8(A) reveals that the pattern of  $i_{s1}$  and  $i_{qs}$  is not same, which highlights the fact that reference frame chosen for this study is other than stator reference frame. Whereas the pattern of  $i_{r1}$  and  $i_{qr}$ as depicted in Figure 9(A) and Figure 10(A) respectively, is same indicating that the reference frame is rotor reference frame (15, 16). Critical observation of stator and rotor flux waveforms as shown in Figure 11(A) and 11(B) reveals that for any change only the stator flux changes in contrast to rotor flux. This further establishes that the reference frame chosen here is the rotor reference frame (15, 16). The offline simulated results have been validated with real-time simulator, OPAL-RT 4510 using HIL with RCP technique. The conversion procedure is given in previous section 2.5. The results obtained with real time simulator are given from Figure 12 to Figure 18.

The congruence of offline rotor speeds illustrated in Figures 5(A), 5(B) with their online counterparts depicted in Figures 12(A), 12(B), alongside the alignment of offline torques represented in Figures 6(A), 6(B) with those in Figures 13(A), 13(B), underscores the practical applicability of the proposed controller. Similarly, offline stator and rotor phase currents displayed in Figures 7(A), 7(B), 7(C) and 9(A), 9(B), 9(C) exhibit a remarkable resemblance to their online equivalents showcased in Figures 14(A), 14(B), 14(C) and 16(A), 16(B), 16(C) respectively. The offline qd stator axes and rotor axes currents illustrated in Figures 8(A), 8(B), and 10(A), 10(B) mirror their online versions presented in Figures 15(A), 15(B) and 17(A), 17(B) respectively. A similar pattern is also evident for the offline and online stator and rotor fluxes (refer to Figures 11(A), 11(B) and 18(A), 18(B)). The congruence of all these variables in both offline and online environments validates the integrity of the conducted work.

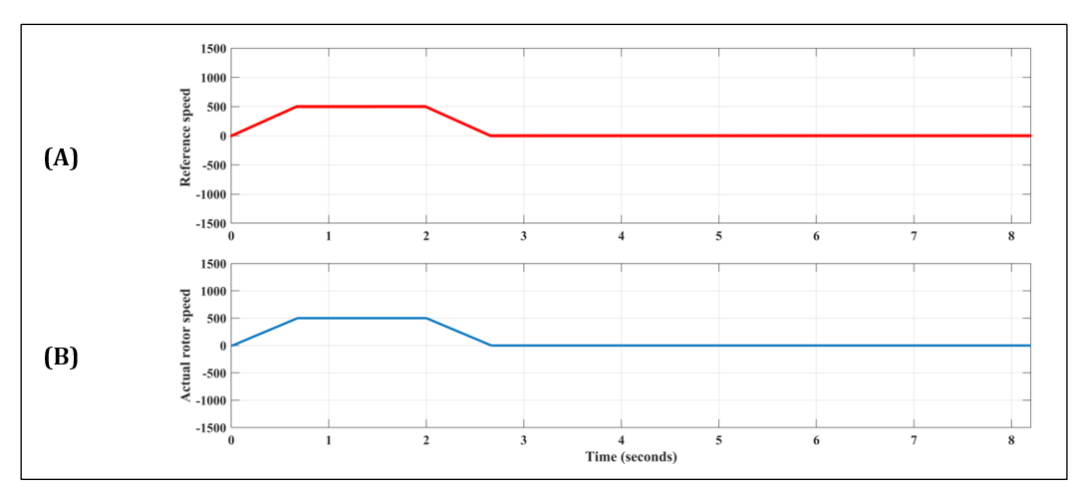


Figure 5: (A) Reference, (B) Actual Rotor Speed Waveforms in Offline Mode

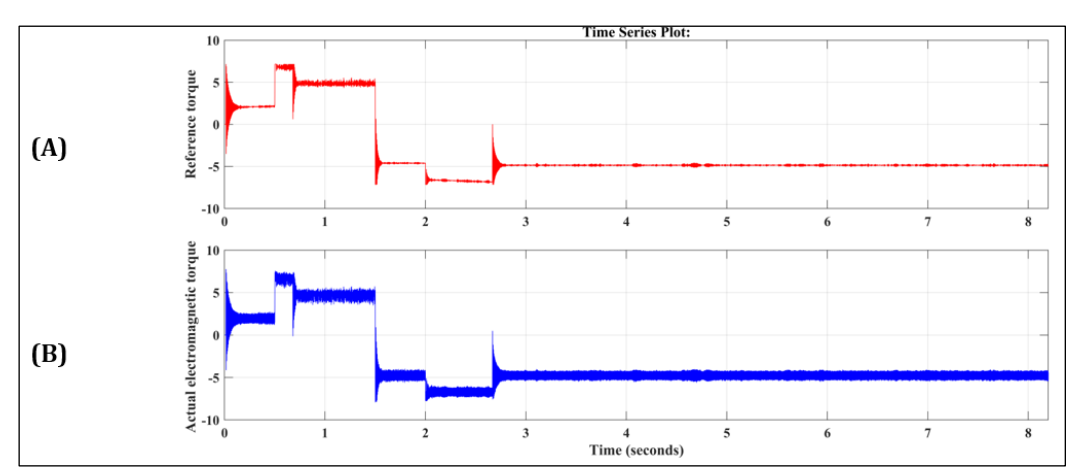


Figure 6: (A) Reference, (B) Electromagnetic Torque Waveforms in Offline Mode

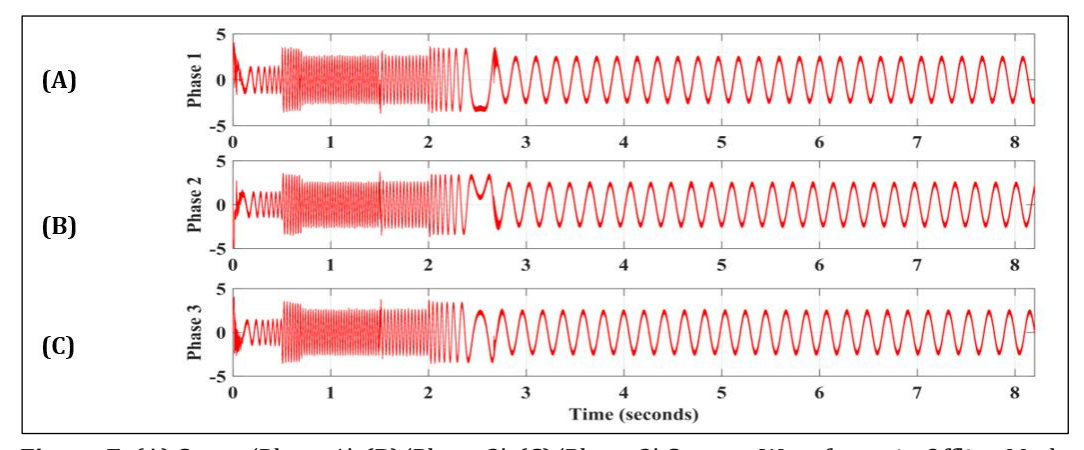


Figure 7: (A) Stator 'Phase 1', (B) 'Phase 2', (C) 'Phase 3' Current Waveforms in Offline Mode

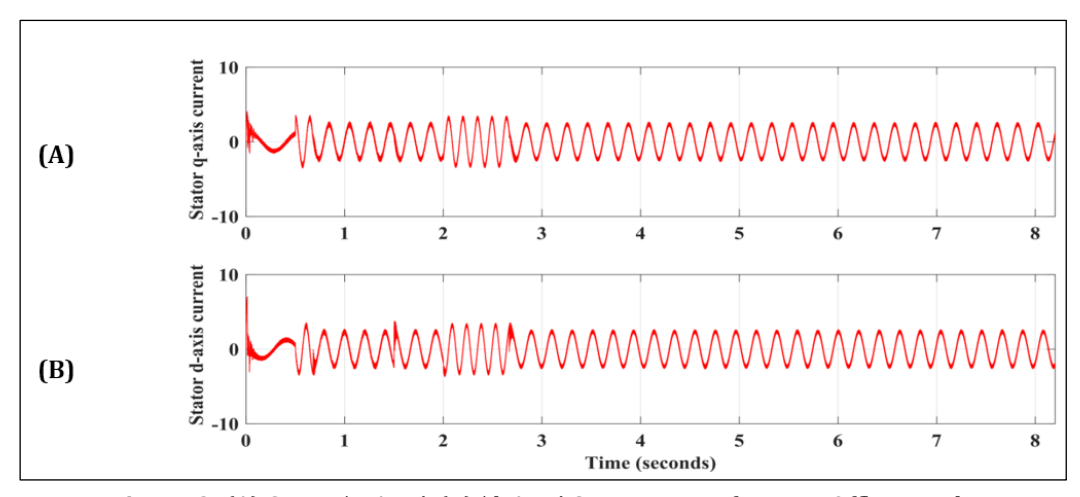


Figure 8: (A) Stator 'q-Axis', (B) 'd-Axis' Current Waveforms in Offline Mode

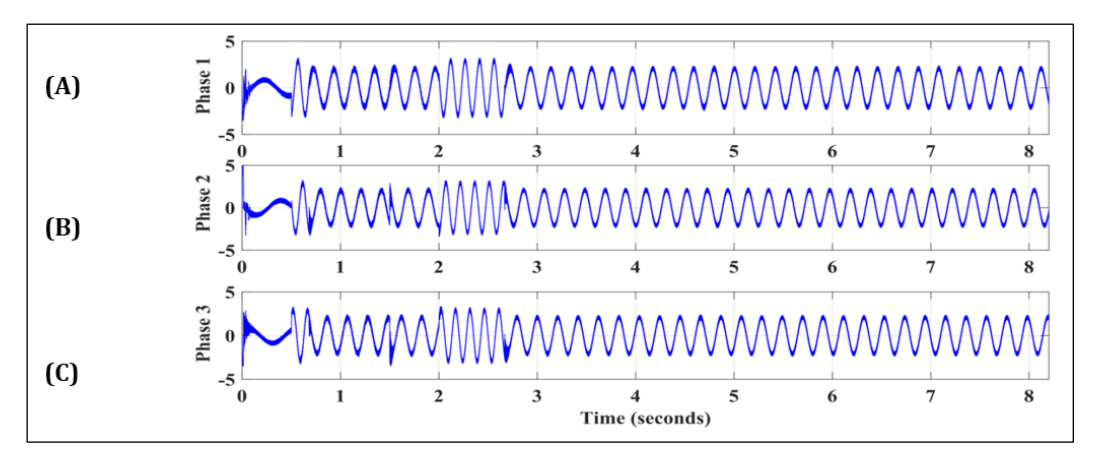


Figure 9: (A) Rotor 'Phase 1', (B) 'Phase 2', (C) 'Phase 3' Current Waveforms in Offline Mode

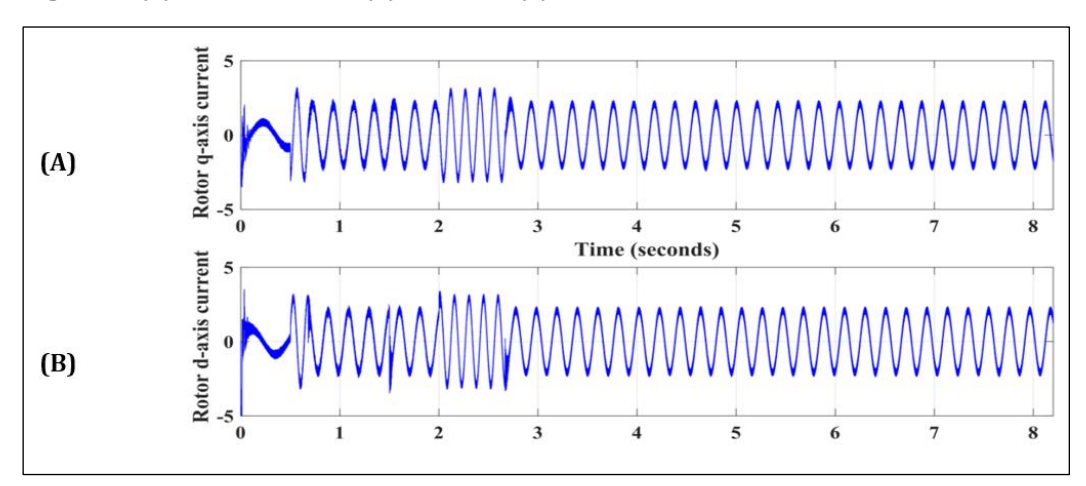


Figure 10: (A) Rotor 'q-Axis', (B) 'd-Axis' Current Waveforms in Offline Mode

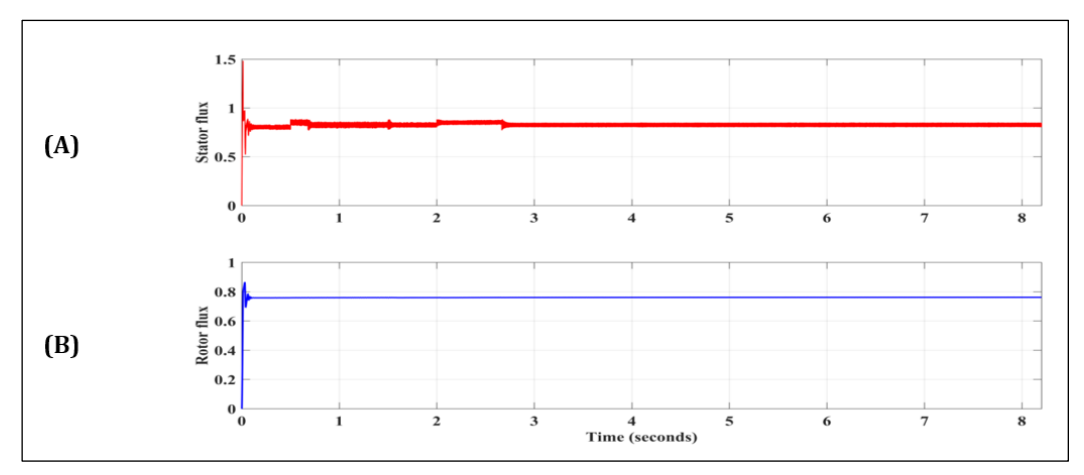


Figure 11: (A) Stator Flux, (B) Rotor Flux Waveforms in Offline Mode

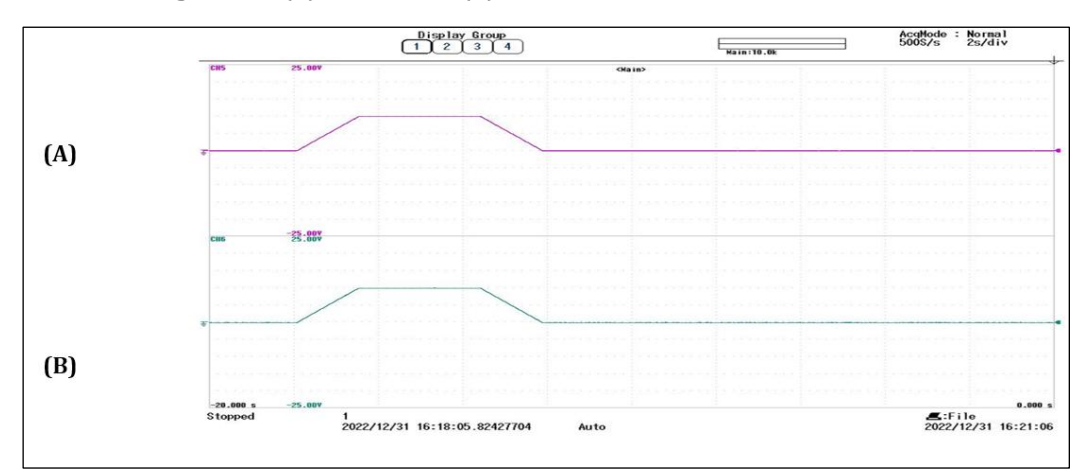


Figure 12: (A) Reference, (B) Actual Rotor Speed Waveforms in Online Mode

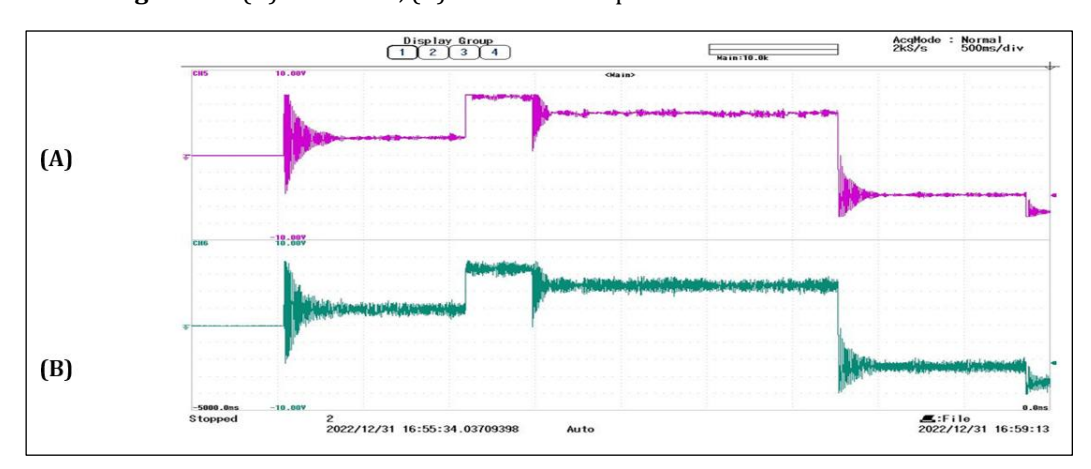


Figure 13: (A) Reference, (B) Electromagnetic Torque Waveforms in Online Mode

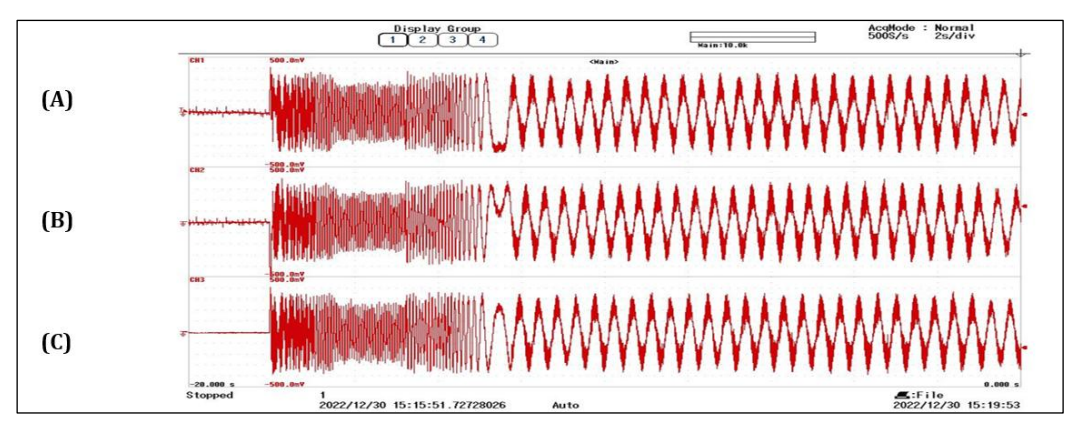


Figure 14: (A) Stator 'Phase 1', (B) 'Phase 2', (C) 'Phase 3' Current Waveforms in Online Mode

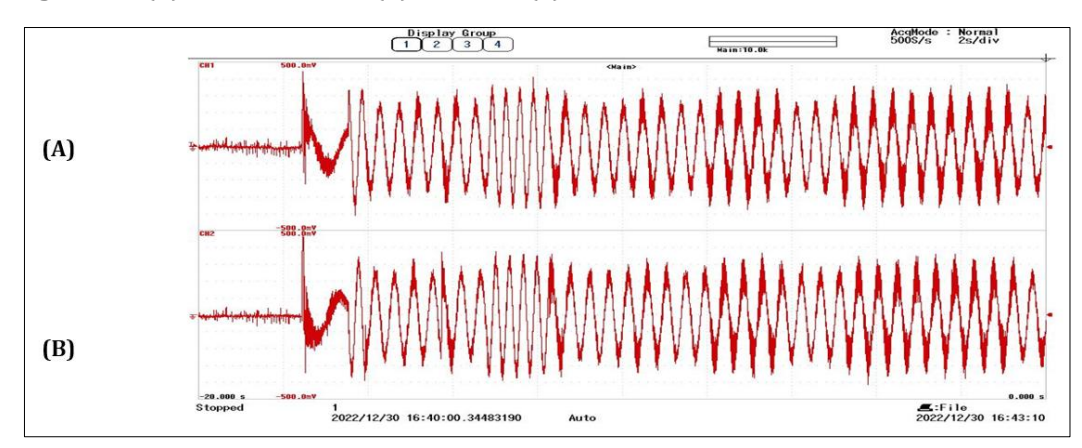


Figure 15: (A) Stator 'q-Axis', (B) 'd-Axis' Current Waveforms in Online Mode

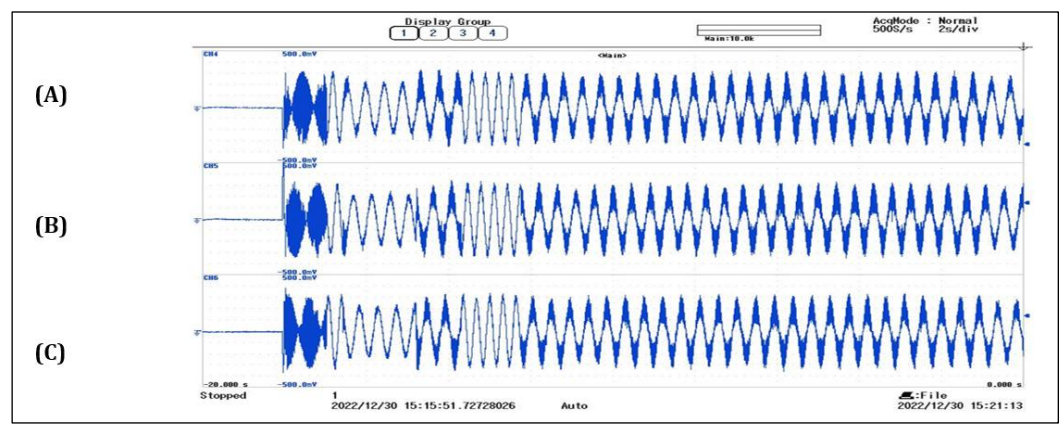


Figure 16: (A) Rotor 'Phase 1', (B) 'Phase 2', and (C) 'Phase 3' Current Waveforms in Online Mode

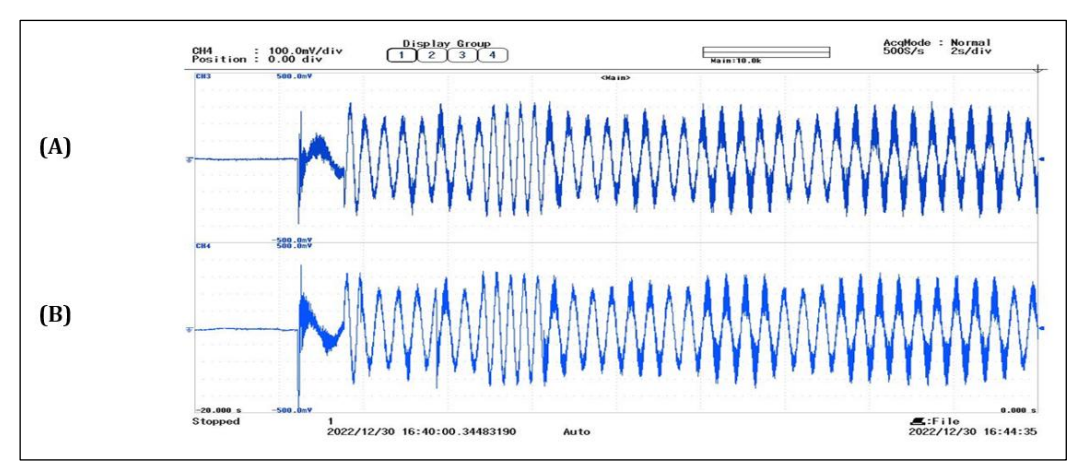


Figure 17: (A) Rotor 'q-Axis', (B) 'd-Axis' Current Waveforms in Online Mode

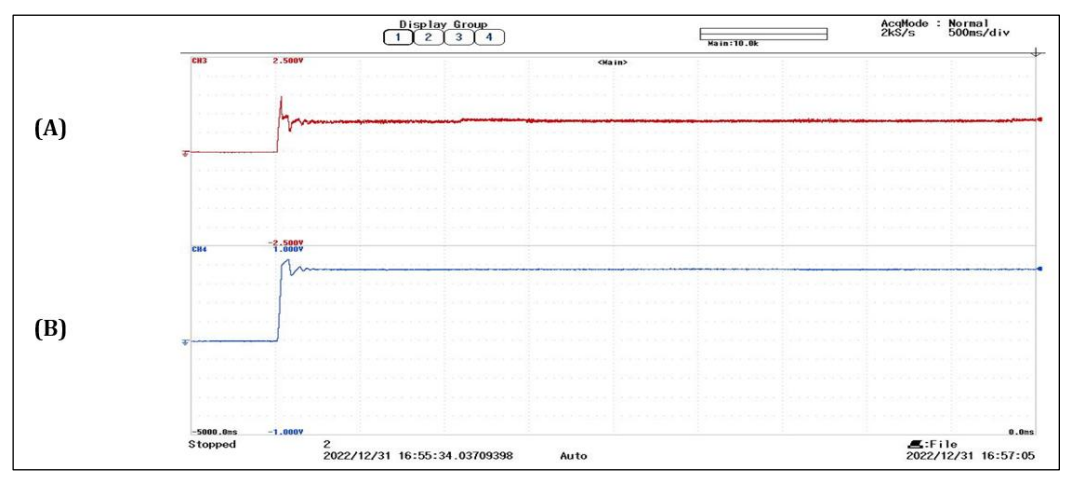


Figure 18: (A) Stator Flux, (B) Rotor Flux Waveforms in Online Mode

It is to be noticed here that although the pattern is same, there is a significant difference in real-time clock and offline simulation w.r.t. time vectors. The time vector in offline environment runs at its own whereas in online environment it is in synchronization with is real-time clock. This can be understood with the help of computation burden. For better understanding, the same model is run in offline environment with three computer systems having different configurations, i.e., i3, i5 and i7 with 8 GB RAMs.

The computational burden,  $\chi$  imposed on the system across various model configurations has been meticulously evaluated in both offline and online environments, as delineated in Table 1, corresponding to a simulation duration of 8.2

seconds. The table unequivocally underscores the disparity in real clock time consumed by computers operating in the offline environment, with configurations i3, i5, and i7 recording times of 351, 240, and 158 seconds, respectively, in stark contrast to the mere 8.2 seconds observed in the online setting. Consequently, the computational burden is calculated to be 42.8, 29.26, and 19.26 times greater for the i3, i5, and i7 computer configurations, respectively. In juxtaposition, the utilization of the real-time simulator (OPAL-RT) significantly alleviates the computational burden to a mere 1, thereby indicating that the control signals generated are impeccably synchronized with the real-time clock (17).

Table 1: Computational Burden in Offline and Online Environment

Environment	Different Systems	Real-clock Time	Computational Burden
		$( au_e)$	$(\chi) = \frac{\tau_e}{8.2}$
Offline	i3	351 sec	42.80 times
	i5	240 sec	29.26 times

	i7	158 sec	19.26 times
Online	OPAL-RT		
	(OP4510)	8.2 sec	1
	real-time	o.z set	1
	simulator		

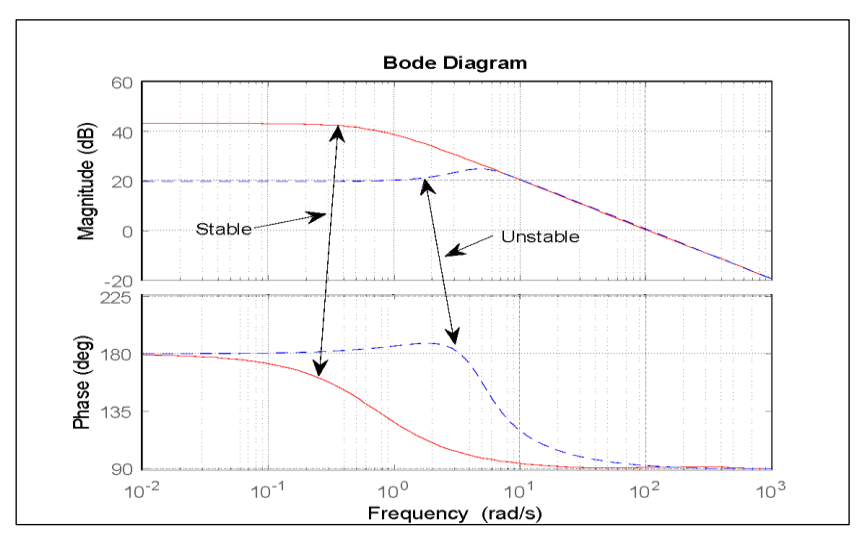


Figure 19: Bode Diagrams of the Induction Machine during Stable and Unstable Mode

Apart from the comprehensive analysis of the induction machine drive system in the time domain, the stability of the machine is assessed through s-domain analysis, as illustrated in Figure 19 (27). The nonlinear machine equations [1] to [5] are linearized around its operating point at 500 rpm (Figure 5) within the MATLAB/SIMULINK environment. The input is the electromagnetic torque, while the output is the rotor speed. The Bode plot demonstrates that the machine exhibits stability with the proposed control strategy (indicated in red), whereas it displays instability in the absence of the controller (depicted in blue).

### **Conclusions**

In this work, a Model Reference Adaptive System (MRAS) based sensor-less vector-controlled induction motor drive system was developed and simulated in both offline and online environments. Furthermore, the machine's stability has also been checked in s-domain. The main objectives of achieving precise speed control and facilitating practical deployment were successfully met. Key conclusions from this study include:

- The proposed scheme demonstrated accurate reference speed tracking during acceleration and deceleration, even at lowest speed.
- The use of acceleration and deceleration scenarios resulted in reduced peak

- currents, potentially lowering inverter ratings and costs.
- The selection of the rotor reference frame was validated by observing the similarity of rotor phase 'a' current and rotor q-axis current, as well as the observed changes in stator flux during load changes while rotor flux remained constant.
- The offline model's computational burden was significantly reduced from approximately 20 times to the required value of one when transformed into an online model using the OPAL-RT 4510 real-time simulator.
- The implementation of the Rapid Control Prototyping (RCP) technique further enhanced the real-time model, minimizing plant stoppage time and improving practical deployment potential.

The proposed control scheme and its real-time implementation offer improved features suitable for existing industries looking for better performance and meet competitive market standards. This approach can help industries to upgrade their systems with minimal disruption, making it particularly valuable in today's competitive environment.

The present study has been conducted on a machine characterized by a low moment of inertia (MOI). The dynamics of control exhibit significant variations with an increase in MOI. Consequently, this limitation can be regarded as a potential avenue for future exploration. Another prospective avenue for this research entails enhancing the precision of the Model Reference Adaptive System (MRAS) based controller through amalgamation of Model Predictive Control (MPC) and model-free Deep Reinforcement Learning (DRL) algorithms. Furthermore, the incorporation of noise, along with its analysis and mitigation, holds paramount significance in such systems. Consequently, this aspect may also be considered a prospective direction for future exploration.

#### **Abbreviations**

ANFIS: Adaptive Neuro-Fuzzy Inference Systems, DRTS: digital real-time simulation, HIL: Hardware-in-the-Loop, MRAS: Model Reference Adaptive System, RCP: Rapid Control Prototyping, RRF: Rotor reference frame.

### Acknowledgement

The author extends his heartfelt gratitude to the Ministry of Environment, Government of India, for bestowing a grant under letter no. 17-11/2015-PN.1, which facilitates the enhancement of research facilities at UIET, Panjab University, Chandigarh, for the establishment of the Design Innovation Center. I am thankful to P. K. Nanda for his valuable suggestions during preparation of the manuscript.

#### **Author Contributions**

Conceptualization, Data curation, Investigation, Writing,-original Draft, review and editing.

#### **Conflict of Interest**

There exists no conflict of interest.

# **Declaration of Artificial Intelligence** (AI) Assistance

The authors declare no use of Artificial intelligence (AI) for the write-up of the manuscript.

## **Ethics Approval**

This article does not encompass any studies involving human participants or animals conducted by the author.

## **Funding**

There is no designated funding allocated for this project.

### References

- Krishnan R. Electric motor and drives: Modeling analysis and control. Original US ed. Upper Saddle River, New Jersey: Pearson Prentice Hall. 2001. https://www.academia.edu/26714897/R\_Krishnan\_ Electric\_Motor\_Drives\_Modeling\_Analysis\_and\_Con\_ trol\_2001
- Lee CHT, Hua W, Long T, et al. A critical review of emerging technologies for electric and hybrid vehicles. IEEE Open J Veh Technol. 2021;2:471–85.
- 3. Fu X, Li S. A novel neural network vector control technique for induction motor drive. IEEE Trans Energy Convers. 2015;30(4):1428–37.
- Wang K, Lorenz RD, Baloch NA. Enhanced methodology for injection-based real-time parameter estimation to improve back EMF selfsensing in induction machine deadbeat-direct torque and flux control drives. IEEE Trans Ind Appl. 2018;54(6):6071–80.
- Reigosa DD, Briz F, Blanco C, et al. Sensorless control of doubly fed induction generators based on stator high-frequency signal injection. IEEE Transactions on Industry Applications. 2014;50(5):3382-91.
- Mohammed OA, Liu Z, Liu S. A novel sensorless control strategy of doubly fed induction motor and its examination with the physical modeling of machines. IEEE Trans Magn. 2005;41(5):1852–5.
- Raute R, Caruana C, Staines CS, et al. Sensorless control of induction machines at low and zero speed by using PWM harmonics for rotor-bar slotting detection. IEEE Trans Ind Appl. 2010;46(5):1989– 98.
- 8. Comanescu M, Xu L. An improved flux observer based on PLL frequency estimator for sensorless vector control of induction motors. IEEE Transactions on industrial electronics. 2006;53(1):50-6.
- Tu X, Hou X, Zhao J, et al. Speed identification of speed sensorless linear induction motor based on MRAS. CES Trans Electr Mach Syst. 2023;7(3):294– 300
- 10. Cardenas R, Pena R. Sensorless vector control of induction machines for variable-speed wind energy applications. IEEE Trans Energy Convers. 2004;19(1):196–205.
- 11. Pena R, Clare J, Proboste J, et al. Sensorless control of doubly-fed induction generators using a rotor-current-based MRAS observer. IEEE Trans Ind Electron. 2008;55(1):330–9.
- 12. Benlaloui I, Drid S, Chrifi-Alaoui L, et al. Implementation of a new MRAS speed sensorless vector control of induction machine. IEEE Trans Energy Convers. 2015;30(2):588-95.
- 13. Govindharaj I, Anandh R, Rampriya R, et al. Improving robustness and dynamic performance of sensorless vector-controlled IM drives with ANFISenhanced MRAS. Int J Electr Electron Res. 2024;12(3):975–80.

- 14. Zbede YB, Gadoue SM, Atkinson DJ. Model predictive MRAS estimator for sensorless induction motor drives. IEEE Trans Ind Electron. 2016;63(6):3511–21
- 15. Lee RJ, Pillay P, Harley RG. D, Q reference frames for the simulation of induction motors. Electric power systems research. 1984 Oct 1;8(1):15-26.
- 16. Prasad RM, Mulla MA. Mathematical modeling and position-sensorless algorithm for stator-side field-oriented control of rotor-tied DFIG in rotor flux reference frame. IEEE Trans Energy Convers. 2020;35(2):631–9.
- 17. Chen J, Yang G, Yuan X, et al. Experimental validation of a minimum-order sensorless induction motor control method. IEEE J Emerg Sel Top Power Electron. 2024;12(4):3715–28.
- 18. Mihalič F, Truntič M, Hren A. Hardware-in-the-loop simulations: a historical overview of engineering challenges. Electronics. 2022;11(15):2462–6.
- 19. Abu Bakar NA, Wan Mohd Jaafar WS, Abdul Maulud KN, et al. Monitoring mangrove-based blue carbon ecosystems using UAVs: A review. Geocarto Int. 2024;39(1):2405123. https://www.tandfonline.com/doi/pdf/10.1080/10
  - https://www.tandfonline.com/doi/pdf/10.1080/10 106049.2024.2405123
- 20. Liang X, Talha M, Pannell J, Su H, Bowes A. A novel OPAL-RT real-time simulator-based experimental approach to study open-switch faults of interfacing inverters of renewable distributed generation in microgrids. IEEE Trans Ind Appl. 2025;99:1-13.

- 21. Karad SG, et al. Optimal design of fractional order vector controller using hardware-in-loop (HIL) and Opal RT for wind energy system. IEEE Access. 2024;12:35033-47.
- 22. Mohamed M, Alaas ZM, Faiya BA, et al. Performance improvement of grid-connected PV-wind hybrid systems using adaptive neuro-fuzzy inference system and fuzzy FOPID advanced control with OPAL-RT. IEEE Access. 2025;13(1):55996-56020.
- 23. Ismeil MA, Alfouly A, Hussein HS, et al. Hardware in the loop real-time simulation of improving hosting capacity in photovoltaic systems distribution grid with passive filtering using OPAL-RT. IEEE Access. 2023;11:78119-34.
- 24. Tasnim MN, Ahmed T, Ahmad S, et al. Implementation of control strategies for energy storage systems and interlinking converters in an interconnected hybrid microgrid system for optimal power management using OPAL-RT. IEEE Trans Ind Appl. 2024;99:1-11.
- 25. Sandhu KS, Pahwa V. Simulation study of threephase induction motor with variations in moment of inertia. ARPN J Eng Appl Sci. 2009;4(6):72–7.
- 26. Ziegler JG, Nichols NB. Optimum settings for automatic controllers. Trans ASME. 1942;64:759-68.
- 27. Nelson RH, Lipo TA, Krause PC. Stability analysis of a symmetrical induction machine. IEEE Trans Power Appar Syst. 1969;88(11):1710-7.

**How to Cite:** Pahwa V. Real-time sensor-less vector control of induction motor drive using model reference adaptive system. Int Res J Multidiscip Scope. 2025; 6(4):935-949. doi: 10.47857/irjms.2025.v06i04.06096